Structural Engineering and Mechanics, Vol. 16, No. 3 (2003) 241-257
DOI: http://dx.doi.org/10.12989/sem.2003.16.3.241

Field testing of a seismically isolated concrete bridge

K. C. Chang†

Department of Civil Engineering, National Taiwan University, Taipei, Taiwan 10617

M. H. Tsai‡

Structural Engineering Department II, China Engineering Consultants, Inc., Taipei, Taiwan 10686

J. S. Hwang†

Department of Construction Engineering, National Taiwan University of Science and Technology, Taipei, Taiwan, 10617

S. S. Wei‡†

Department of Civil Engineering, National Taiwan University, Taipei, Taiwan 10617

(Received June 25, 2001, Revised February 22, 2003, Accepted June 3, 2003)

Abstract. The first seismically isolated structure in Taiwan was completed in early 1999. Seven new bridges of the Second National Freeway located at Bai-Ho area, a region which is considered to be of high seismic risk, have been designed and constructed with lead-rubber seismic isolation bearings. Since this is the first application of seismic isolation method to the practical construction in Taiwan, field tests were conducted for one of the seven bridges to evaluate the assumptions and uncertainties in the design and construction. The test program is composed of ambient vibration tests, forced vibration tests, and free vibration tests. For the free vibration tests, a special test setup composed of four 1000 kN hydraulic jacks and a quick-release mechanism was designed to perform the function of push-and-quick release. Valuable results have been obtained based on the correlation between measured and analytical data so that the analytical model can be calibrated. Based on the analytical correlation, it is concluded that the dynamic characteristics and free vibration behavior of the isolated bridge can be well captured when the nonlinear properties of the bearings are properly considered in the modeling.

Key words: bridge; seismic isolation; lead-rubber bearings; field tests.

1. Introduction

Seismic isolation technology has been successfully applied to protect civil engineering structures

† Professor
‡ Engineer
‡† Graduate Research Assistant

against earthquake loading over the past two decades. Excellent performances of some isolated structures during the 1994 Northridge and 1995 Hyogoken Nanbu earthquakes have been reported and documented (Asher *et al.* 1997). It is of particular interest that a few field tests on seismically isolated bridges have been conducted in the recent years (Gilani *et al.* 1995, Wendichansky 1996, Chen *et al.* 1998, Ronson and Hark 1998). A good example of success is the field test of the Walnut Creek Viaduct in California (Gilani *et al.* 1995). The test program in that study, including the ambient, forced, and free vibration tests, was conducted for a couple of bridge columns and the complete bridge.

The first practical application of seismic isolation in Taiwan was completed in 1999. Seven new bridges located in the Bai-Ho area, a region where major earthquakes occurred several times in the past century, have been designed and constructed with lead-rubber seismic isolation bearings. Since this is the first application of seismic isolation technology in Taiwan, it is of academic and practical interests to conduct a series of field tests for one of the seven isolated bridges. The major objectives of the field testing were to experimentally verify the targeted design philosophy of the seismically isolated bridge and to calibrate analytical models for future analytical correlation and prediction.

In this paper, the field tests conducted on the Bai-Ho bridge are presented. The test program includes ambient, forced and free vibration tests on the bridge. A specially designed quick-release setup with four 1000 kN hydraulic jacks was used for the free vibration tests. The testing method was different from those used by other researchers (Gilani *et al.* 1995, Wendichansky 1996, Chen *et al.* 1998, Ronson and Hark 1998), in which explosion or mechanical fuse were used for the quick release of the tensioned cables. Based on the test results, an analytical model constructed using SAP2000 (1995) was used to simulate the dynamic characteristics of the seismically isolated bridge. This analytical model can be further applied to the future seismic response prediction of the isolated bridge.

2. Description and design of the Bai-Ho bridge

The bridge is located at the milepost of 221 km + 736 on the northbound of the Second National Freeway overpassing the Chia-Nan canal. The superstructure is a non-prismatic, prestressed concrete box-girder continuous over three spans. The span lengths are 40 m, 65 m, and 40 m, as shown in Fig. 1. The substructure is composed of two column bents and abutments sitting on pile

Fig. 1 An overview of the seismically isolated Bai-Ho bridge

Fig. 2 The lead-rubber bearings used on the bridge

foundations. Above each column bent, two lead-rubber bearings (LRBs), each with a plan dimension of 1250 mm × 1250 mm and a height of 247 mm, were installed. Details of the bearings are illustrated in Fig. 2. PTFE coated rubber bearings were used at the two abutments. However, shear keys and specially designed steel rods were provided on the abutment to restrict the transverse movement of the superstructure. Therefore, the bridge is completely isolated only in the longitudinal direction while it is partially isolated in the transverse direction.

Similar to the design practices in the United States and Japan, the displacement-based method is used for the design of seismic isolated bridges. The theoretical background is that the inelastic displacement response spectra of a ground motion can be approximated by the elastic displacement spectra if the equivalent damping ratio and effective stiffness (effective period) can be appropriately considered. Based on an iteration procedure (Hwang *et al.* 1995), the design displacements of the isolated bridge and the isolation bearings can be determined. Once the design displacement of isolation bearing is determined, design seismic forces acting on the bridge can be easily calculated based on the hysteresis characteristics of the bearings.

For the design of the Bai-Ho bridge, an effective peak ground acceleration of 0.33 g and an importance factor I of 1.35 are used for determining the 5% damped elastic design spectra. Based on the aforementioned analysis method, the design requirements are prescribed and the design parameters are calculated as follows:

1. Direction of isolation: longitudinal and partially transverse.
2. Isolation period: longitudinal 2.04 sec, transverse 0.85 sec
3. Bearing design parameters:
   Dead load (DL): 9005.6 kN
   Dead load + live load (DL + LL): 10614.4 kN
   Seismic lateral force: 1347.9 kN
   Seismic design displacement: 12.5 cm
   Non-seismic lateral force: 309.0 kN
   Non-seismic design displacement: 0.6 cm
   Maximum expected rotation in the superstructure structure: 0.004 rad
4. Design specifications for the LRBs:
   Effective stiffness K_{eff} = 10791 kN/m
   Energy dissipation capacity EDC = 175.6 kN-m

3. Test program and results

One of the purposes of the field tests is to assess the assumptions made in the design and, if necessary, to modify the design method for future applications to seismically isolated bridges in Taiwan. Results from the ambient and forced vibration tests will provide the dynamic characteristics of the bridge under normal loads and frequent minor earthquakes. While the free vibration tests are used to investigate the dynamic behavior of the bridge under small-to-moderate earthquakes.

3.1 Performance test of bearings

Before the LRBs were installed to the bridge, a series of cyclic loading tests were conducted by the supplier to ensure that the characteristics of the bearings meet the design requirements. The bearing tests specified in the isolation design guidelines of Taiwan include the qualification test and performance test. The manufacturers are not allowed to produce all bearings listed in each purchase order until two prototype bearings have passed the qualification test and conformed with the design mechanical characteristics. In addition, before the bearings are installed to the structure, the performance test has to be conducted on each bearing to show that the bearings satisfy the design requirements.

The performance test requires that, under the design dead load, three cycles of lateral displacement reversals with a maximum value equal to the design displacement of the bearing should be carried out. The average effective stiffness should not differ more than 15% from the design value. The average energy dissipation capacity (EDC) should not be less than 85% of the design EDC. A typical test result of the LRB installed to the Bai-Ho bridge is shown in Fig. 3 and summarized in Table 1. From the table, it is clear that the equivalent linear characteristics determined corresponding to the design displacement of the isolation bearings satisfied the design specifications.

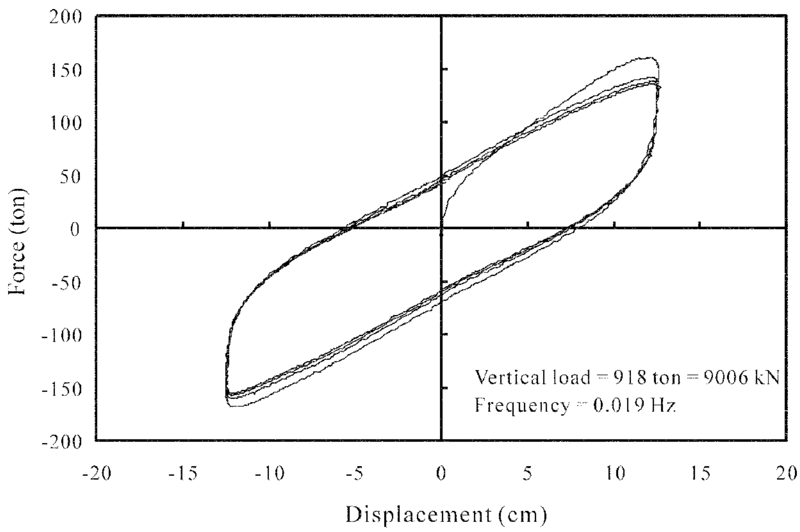

Fig. 3 Hysteresis loop of LRB at design displacement

Table 1 Results of the performance test of LRB at the design displacement

Rubber area = 14689 cm^2, Vertical load = 918 ton*, Rubber thickness = 15.0 cm, Frequency = 0.019 Hz											
Loop	Shear force (ton)		Displacement (cm)		EDC (ton-m)	Strain (%)	K_{eff} (ton/m)	Q_d (ton)	K_r (ton/m)	G (ton/m^2)	Damping (%)
	Min.	Max.	Min.	Max.							
1	−161.3	167.8	−12.5	12.6	28.56	84	1311.3	58.6	844.0	86.2	22.0
2	−153.7	149.3	−12.5	12.6	26.62	84	1207.4	53.4	782.2	79.9	22.3
3	−150.3	145.3	−12.5	12.8	25.35	84	1171.1	51.8	761.0	77.7	21.6
4	−148.5	143.1	−12.5	12.6	24.63	84	1162.1	49.6	767.1	78.3	21.4
Average	−150.8	145.9	−12.5	12.7	25.53	84	1180.2	51.6	770.1	78.6	21.8
	148.4		12.6								

'*' 1 ton = 9.81 kN

Note: Q_d = characteristic strength, K_r = post stiffness, and G = shear modulus of the bearing

3.2 Ambient vibration test

Ambient vibration tests were first conducted on the footing and the bent cap before the construction of superstructure. After the completion of the superstructure, the ambient vibration tests were also carried out on the bridge deck and the top of the pier to identify the fundamental dynamic characteristics of the whole bridge. Ambient vibration responses in the longitudinal, transverse, and vertical direction of the bridge were measured in a sequential order. Fig. 4 shows that eight acceleration sensors are arranged to measure the ambient vibration responses in the lateral direction.

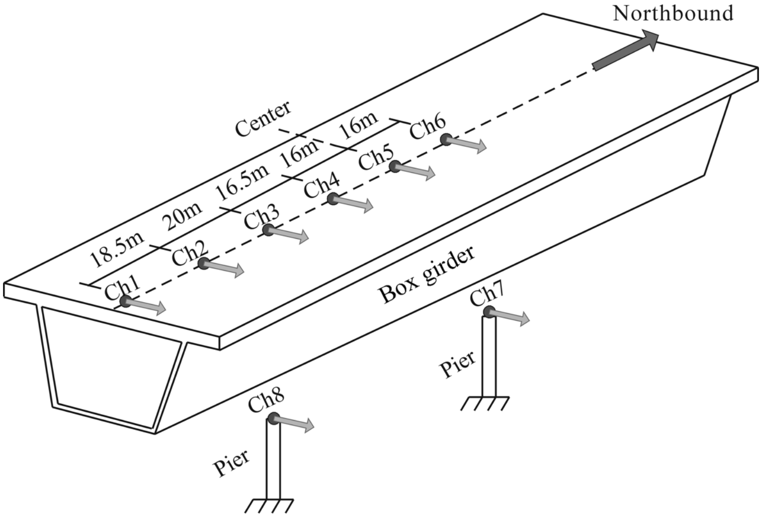

Fig. 4 Distribution of sensors for transverse ambient vibration test

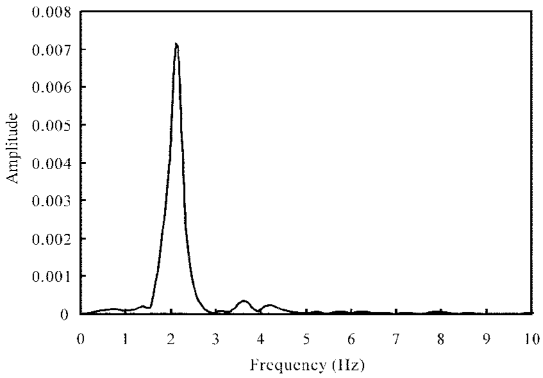

Fig. 5(a) Longitudinal frequency response of the isolated bridge at channel 5

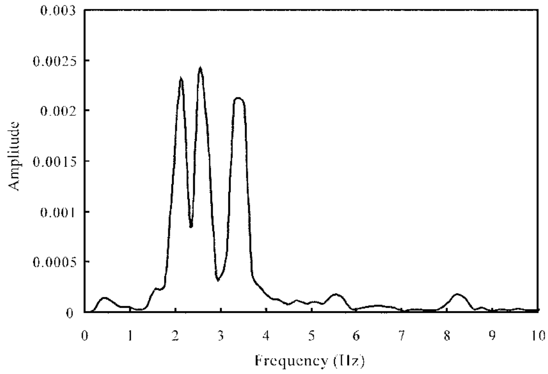

Fig. 5(b) Lateral frequency response of the isolated bridge at channel 5

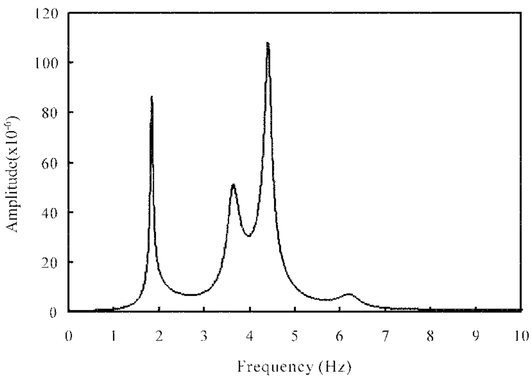

Fig. 5(c) Vertical frequency response of the isolated bridge at channel 2

Considering the symmetric configuration of the bridge, five sensors were distributed on one half of the bridge deck from channel 1 to channel 5. Channels 2 and 5 are approximately located at the center of the end and central spans, respectively. Channels 7 and 8 are located on the top of piers. Similar sensor layouts were used for the other two directions. During the test, data acquisition was proceeded for five minutes at a sampling rate of 100 Hz in each direction.

Typical frequency responses of the bridge under the ambient vibration are shown in Figs. 5(a), 5(b), and 5(c). Figs. 5(a) and 5(b) show respectively the longitudinal and transverse frequency responses that are deduced from the data measured at channel 5. It is seen that the first vibration frequency is approximately equal to 2.1 Hz in those two horizontal directions. Fig. 5(c) shows the frequency response in the vertical direction based on the measured data of channel 2, from which the first vibration frequency is determined to be 1.86 Hz.

Extracting the modal amplitudes from the frequency response obtained from each channel, the mode shapes of the superstructure under ambient vibration can be plotted. Figs. 6(a) and 6(b) show the second and the first mode shape in the transverse and the vertical direction, respectively. From Fig. 6(a), it is observed that the transverse amplitude at the abutment is not equal to zero even though the bridge was designed to be restrained transversely at the abutment. This is because that a

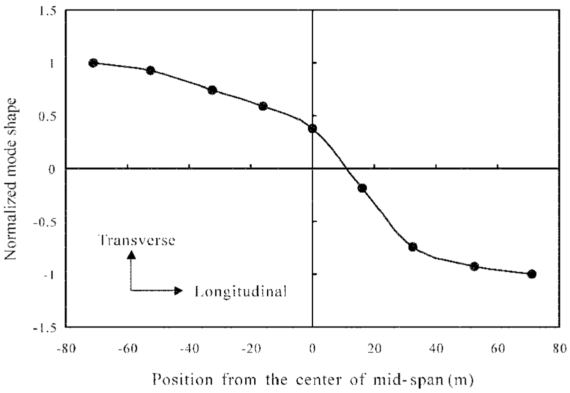

Fig. 6(a) The lateral mode shape at 2.54 Hz from the ambient vibration test

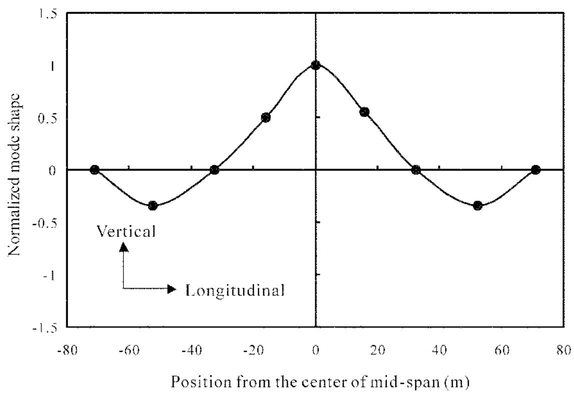

Fig. 6(b) The vertical mode shape at 1.86 Hz from the ambient vibration test

Table 2 The first few modal frequencies of the bridge from test results and analysis

Item	Direction	1st mode	2nd mode	3rd mode
Ambient vibration	Longitudinal	2.12 Hz		
	Transverse	2.15 Hz	2.54 Hz	3.51 Hz
	Vertical	1.86 Hz	3.69 Hz	4.45 Hz
Forced vibration	Longitudinal	2.0 Hz		
	Transverse	2.02 Hz		3.16 Hz
	Vertical			4.38 Hz
Analysis (SAP2000)	Longitudinal	2.042 Hz		
	Transverse	2.261 Hz	2.468 Hz	3.361 Hz
	Vertical	1.864 Hz	3.711 Hz	4.995 Hz

small gap between the shear key and the superstructure at the abutment is provided to accommodate possible transverse movement of the superstructure during daily traffic, and the response amplitude at the deck end is much smaller than the gap provided under the ambient vibration. The fundamental characteristics of the bridge determined from the ambient vibration tests are summarized in Table 2.

3.3 Forced vibration test

Forced vibration tests using two rotating-mass shakers, as shown in Figs. 7(a) and 7(b), have been carried out on the bridge deck after the construction of the superstructure was completed. As presented in Table 3, these shakers can be precisely controlled over a wide frequency range to estimate the fundamental dynamic characteristics of the bridge under normal traffic and minor earthquake conditions. The shakers were mounted on the center of the mid-span and harmonically dynamic loading was applied respectively in the longitudinal, transverse and vertical directions.

Fig. 7(a) The horizontal vibration shaker

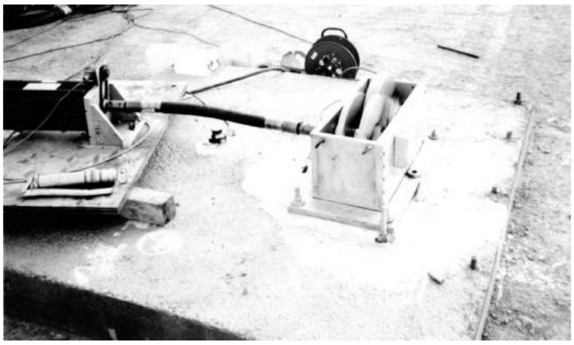

Fig. 7(b) The vertical vibration shaker

Table 3 Characteristics of the vibration shakers

Characteristics \ Type	MK-12.8-4600	MK-12-460
Frequency range (Hz)	0.5-10	0.5-30
Maximum torque (N-m)	521	52
Maximum output force (kN)	49	49
Minimum operation frequency at maximum output force (Hz)	4.6	14.6
Precision	0.5%	0.5%
Synchronization	Yes	Yes
Weight (N)	7548.8	1672.6
Dimension	1 m × 1.5 m × 0.3 m	0.6 m × 0.6 m × 0.3 m
Output direction	Horizontal	Vertical

A total of 15 velocity sensors are used to measure the response of the bridge for the lateral direction, as shown in Fig. 8(a), and 13 velocity sensors are used in the vertical direction, as shown in Fig. 8(b). The arrangement of these sensors is similar to that of the ambient vibration test. Channel 10 and channel 9 are located at the mid-span center to measure the horizontal and vertical forced excitations, respectively.

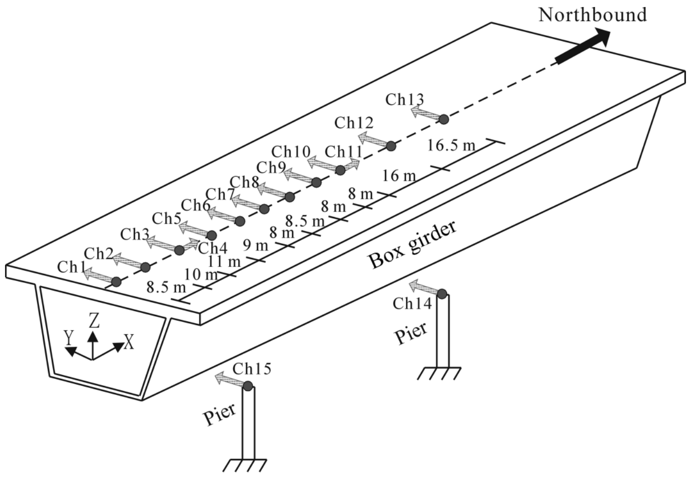

Fig. 8(a) Distribution of the velocity sensors for transverse forced vibration test

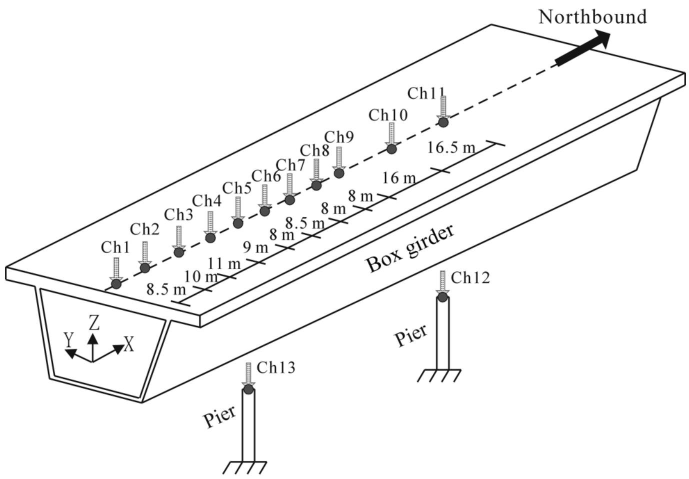

Fig. 8(b) Distribution of the velocity sensors for vertical forced vibration test

Figs. 9(a) and 9(b) show the longitudinal and transverse frequency responses obtained from the measured data of channel 10. The first resonant frequency is equal to 2.0 Hz in both directions. The vertical frequency response deduced from channel 9 is shown in Fig. 9(c). Because the capacity of the vertical shaker is much smaller than that of the horizontal shaker, there is only one resonant frequency obtained at 4.38 Hz in the vertical direction. In a similar way, the mode shapes of the bridge deck under the harmonic vertical vibration can be estimated as shown in Figs. 10(a) and 10(b). In order to obtain the mode shapes under a constant excitation force, the measured structural response is normalized by the square of the excitation frequency for each test. The fundamental dynamic characteristics obtained from the forced vibration tests are summarized in Table 2. It should be pointed out that the second resonant frequency in the transverse direction was not detected because the shaker was located at the nodal point of that vibration mode.

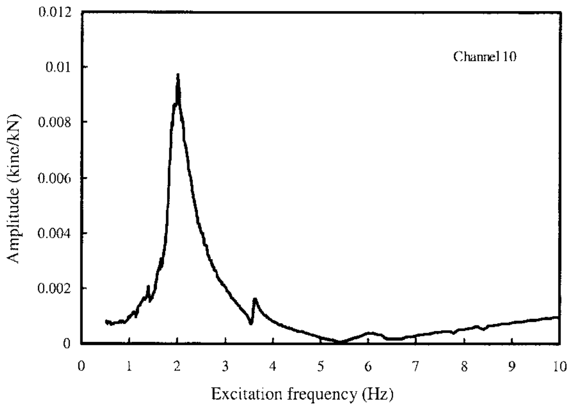

Fig. 9(a) Longitudinal frequency response from the longitudinal forced vibration test

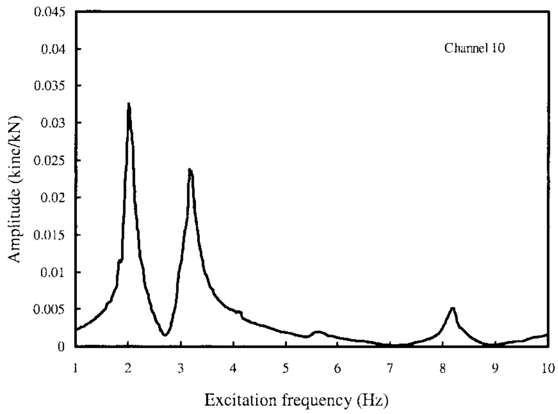

Fig. 9(b) Transverse frequency response from the transverse forced vibration test

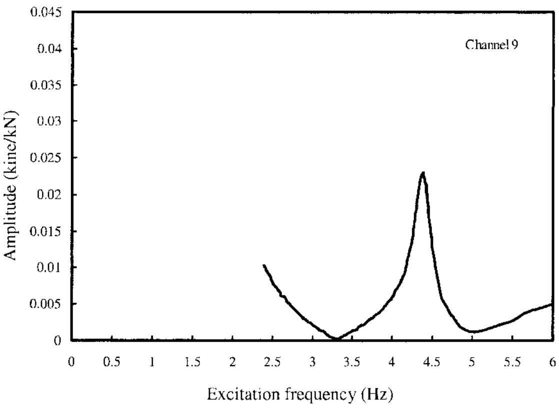

Fig. 9(c) Vertical frequency response from the vertical forced vibration test

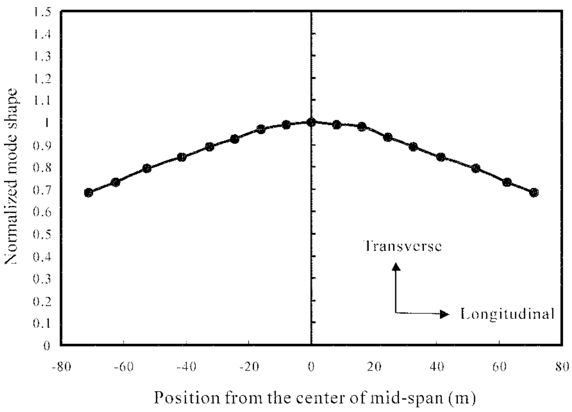

Fig. 10(a) The transverse mode shape at 2.02 Hz from the forced vibration test

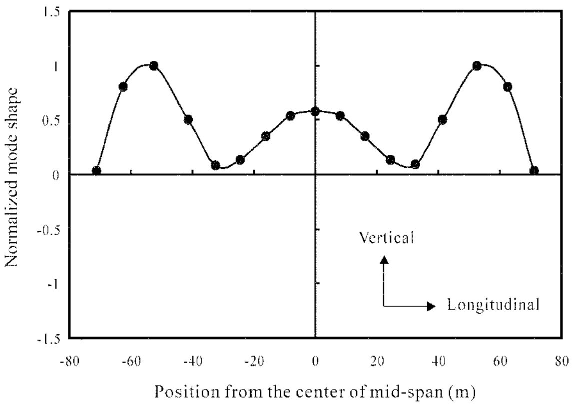

Fig. 10(b) Vertical mode shape at 4.38 Hz from the forced vibration test

3.4 Free vibration test

The free vibration tests are conducted by pushing the bridge deck along its longitudinal axis using four hydraulic jacks with a full load capacity of about 4000 kN, as shown in Fig. 11. The hydraulic jacks have been mechanically modified so that they can be free to move after the hydraulic oil is quickly released. Because the abutments of the bridge were designed mainly to carry the vertical reactions transmitted by the bearings of the abutment, they may not have a sufficient stiffness or strength to support the hydraulic jacks to push the bridge deck. A reinforced concrete reaction wall was therefore constructed as a temporary structure for the loading system. This reaction wall and the back-filled soil on one side of the reaction wall provide the lateral resistance to the hydraulic jacks while pushing the bridge deck to move. The maximum imposed displacement to the bridge deck is gradually increased during the tests, as shown in Table 4. Five accelerometers and ten dial gauges are used to measure the free vibration response of the bridge, as shown in Fig. 12. The information obtained from these tests could more or less represent the inelastic response characteristics of the bridge bearings during a small to moderate earthquake.

During the tests, because of the jack capacity, the maximum displacement imposed on the bridge deck was 2.3 cm, which is only slightly smaller than 2.5 cm. The maximum jack force was approximately equal to 3812 kN. This maximum imposed displacement is well beyond the bearing's yielding point, according to the results of the performance tests of the bearings described

Fig. 11 Four hydraulic jacks used in the free vibration test

Table 4 Estimated frequency and damping ratio from the free vibration test

Maximum displacement (cm)	0.5	0.8	1.5	2.5
Jack force (kN)	1452	2186	2915	3812
Natural frequency (Hz)	1.18	1.11	1.01	0.93
Damping ratio (%)	5.3	9.5	11.3	17.1

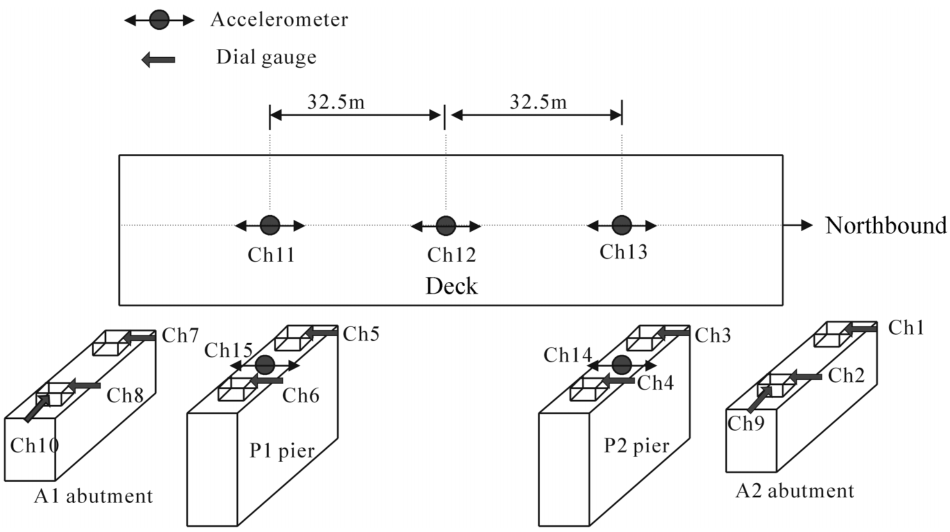

Fig. 12 Distribution of sensors for the free vibration test

earlier. A typical measured response of the LRB is shown in Fig. 13(a). Equivalent viscous damping ratios are calculated using the log-decrement method for the free vibration tests (Clough and Penzien 1993, Chopra 1995). The method is applied to the positive displacement peaks of each test. The identified vibration frequencies and damping ratios obtained from the tests are summarized in Table 4.

In addition, a comparison between the measured accelerations at the deck and the bent cap is made in Fig. 13(b). It is seen that the acceleration of the bent cap is much smaller than that on the deck, clearly demonstrates the effectiveness of the isolation bearings.

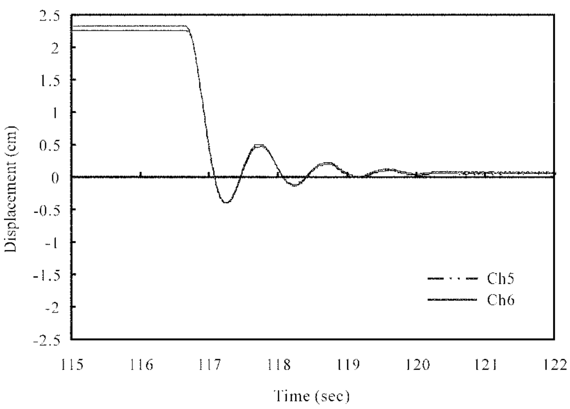

Fig. 13(a) Displacement time history of the lead-rubber bearings

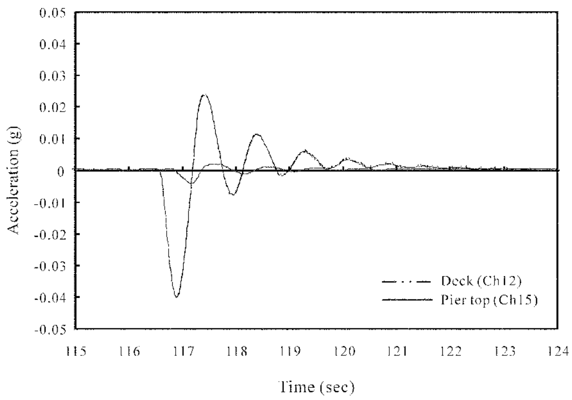

Fig. 13(b) Comparison of the deck and the pier top acceleration time histories

4. Numerical simulation

A finite element model for the bridge is constructed using a commercially available program, SAP2000 (1995). The superstructure is a continuous non-uniform section beam system, which is modeled as step-wise line elements with different sectional properties. The total weight of the superstructure is about 42000 kN. Between the superstructure and the pier are the LRBs, which are represented by a linear viscous damper and a rubber isolator using the "NLLlink" elements in the SAP2000 program. The rubber isolator exhibits a bilinear hysteretic behavior in two horizontal directions and linear elastic behavior in the vertical direction. The bearings at the abutment are modeled by the sliding type isolators. Gap elements are also modeled in both the longitudinal and transverse directions to simulate the space provided for the thermal expansion joints and shear keys. These gap elements are not effective in simulating the ambient vibration tests because the displacement under ambient vibration is much smaller than the gaps. A schematic representation of the bearing models is shown in Figs. 14(a) and 14(b).

From the test results, it is observed that the dynamic characteristics of the isolated bridge are quite different under various levels of vibration (Chang *et al.* 2000). Thus, the parameters of the bearing models may have to be estimated based on the magnitude of vibration.

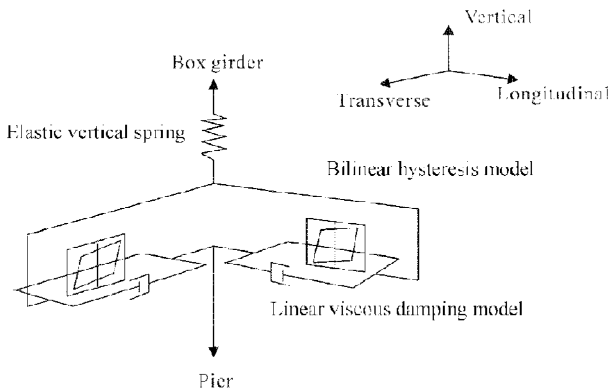

Fig. 14(a) Modeling of the lead-rubber bearings

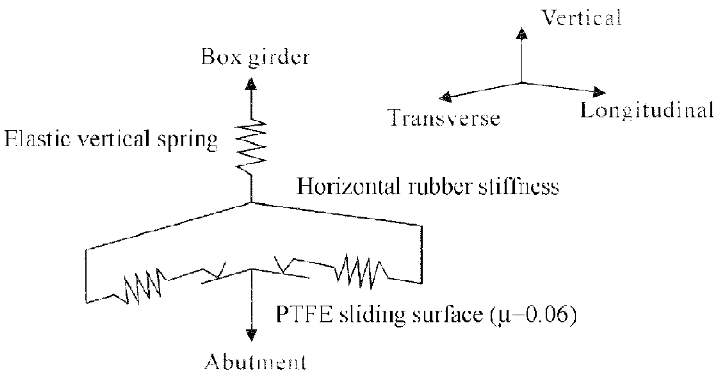

Fig. 14(b) Modeling of the PTFE rubber bearings

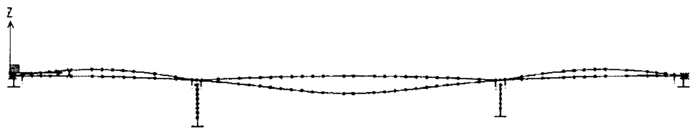

(a) 1st mode, T=0.5365 sec (f = 1.864 Hz) Vertical bending

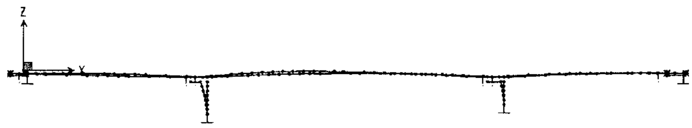

(b) 2nd mode, T=0.4897 sec (f = 2.042 Hz) Longitudinal

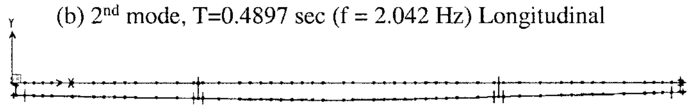

(c) 3rd mode, T=0.4422 sec (f = 2.261 Hz) Transverse translation (Top view)

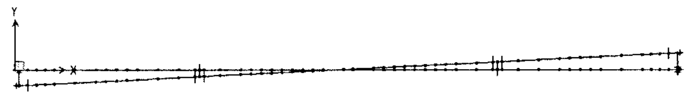

(d) 4th mode, T=0.4052 sec (f = 2.468 Hz) Transverse rotation (Top view)

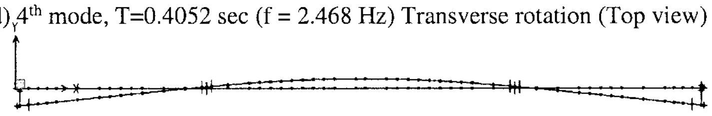

(e) 5th mode, T=0.2975 sec (f = 3.361 Hz) Transverse bending (Top view)

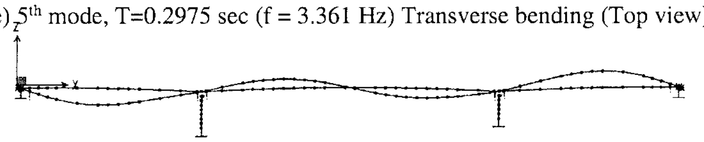

(f) 6th mode, T=0.2695 sec (f = 3.711 Hz) Vertical bending 2

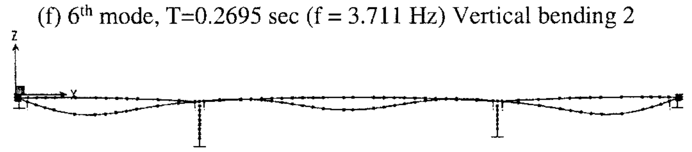

(g) 7th mode, T=0.2002 sec (f = 4.995 Hz) Vertical bending 3

Fig. 15 The calculated modal frequencies and mode shapes of the first few modes

4.1 Ambient vibration

The bearing properties are modeled based on the full-scale component tests to simulate the dynamic characteristics under ambient vibration. Based on the criterion of equal dissipated energy in one cycle, the estimated elastic stiffness of the LRB model from the component tests under 4 mm displacement is 70.0 MN/m. When compared with the ambient vibration tests, it is found that the natural period is overestimated. Since rubber is a highly nonlinear material, the tangent stiffness of the LRB varies with deformation. Hence, the initial tangent stiffness estimated from the component tests is used to model the elastic stiffness of the bearings. The initial tangent stiffness used is 155.0 MN/m for the LRB. Fig. 15 shows that the calculated modal frequencies and modal shapes of the first few vibration modes are consistent with the results from the ambient vibration tests. The measured and calculated modal frequencies are listed in Table 2.

4.2 Free vibration

As observed from the simulation of ambient vibration behavior, the bearing properties indeed depend on the magnitude of vibration. Hence, it is expected that the bearing properties used in the simulation of free vibration should be determined based on the imposed displacement. According to the result of bearing tests, the bilinear behavior of the LRB is not apparent under a small displacement. In the case of the maximum imposed displacement (2.5 cm), the horizontal elastic stiffness and post-elastic stiffness ratio of the LRB from an approximately bilinear loop is estimated to be 41.0 MN/m and 0.7, respectively. The elastic stiffness of the rubber bearings at the abutments is equal to 19.3 MN/m. Besides, 2% inherent damping ratio is assumed for the superstructure and 3% is used in the linear viscous damping element to account for the small damping ratio provided by the rubber material.

Fig. 16(a) shows the simulated result of the displacement response for the free vibration test at the maximum imposed displacement. It is seen that the free vibration behavior of the isolated bridge is accurately captured except for the first peak. The difference at the first peak appears to be the result of pounding of the bridge deck and the hydraulic jacks. Since those jacks are actuated by a hydraulic system, they could not immediately move back to their starting position even though the hydraulic oil was quickly released at that moment. This can be confirmed by comparing the measured acceleration response to the simulated result, as shown in Fig. 16(b). It is observed that there is a phase lag between the two acceleration time histories. Also, an ideal acceleration response of free vibration should exhibit an abrupt jump at the time of quick release, as observed in the numerical simulation. Thus, it is believed that the superstructure pushed the hydraulic jacks at the first half cycle, such that those jacks performed as an additional damping system to mitigate the structural response.

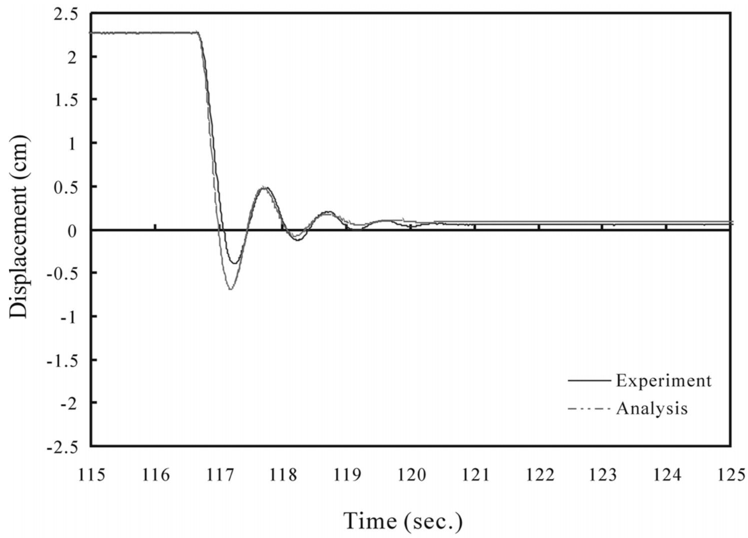

Fig. 16(a) Simulation on the displacement response of the free vibration test

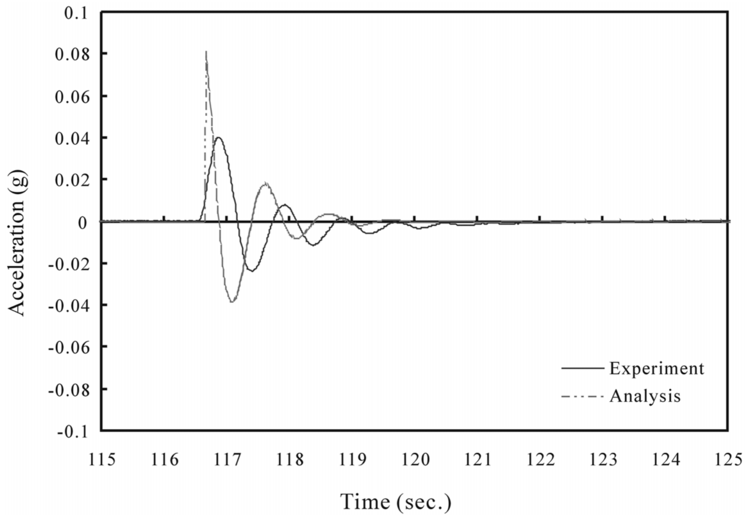

Fig. 16(b) Simulation on the acceleration response of the free vibration test

5. Conclusions

Field tests have been carried out on a seismically isolated bridge. The tests include ambient vibration tests, forced vibration tests and free vibration tests. The free vibration tests are conducted by the quick release of an imposed displacement to the bridge deck. Valuable results have been obtained for analytical correlation and are used to determine the numerical model. It is realized that the dynamic properties of the bearings are highly nonlinear and depend on the magnitude of vibration. The dynamic characteristics of the isolated bridge under ambient vibration are well captured when the nonlinear property of the bearings is considered in the modeling.

Besides, unexpected pounding of the bridge deck and the hydraulic jacks occurred at the first half cycle response of the free vibration tests. Based on the dynamic properties of bearings estimated at the imposed displacement, the free vibration behavior of the isolated bridge is well simulated after the first half cycle. However, it reveals that the seismic response of the isolated bridge under small earthquakes may not be accurately predicted by using the mechanical properties of the LRBs at the design displacement. An appropriate estimation of the mechanical properties of the LRBs at a smaller displacement may be necessary in the design procedure to predict the performance of the isolated bridge under small earthquakes.

Acknowledgements

The work presented in this paper is funded by China Engineering Consultants Inc. (CECI) through the National Expressway Engineering Bureau of Taiwan. This support is gratefully acknowledged. The National Center for Research on Earthquake Engineering (NCREE) and the Department of Civil Engineering of the National Taiwan University provided various test facilities for this test. The assistance by Mr. S.C. Lin of NCREE for the ambient and forced vibration tests and Mr. H.W. Chen of National Taiwan University for the free vibration test are greatly appreciated. The engineers from CECI and Hsin-Yia Construction Company have also contributed greatly to this project during the field tests.

References

Asher, J.W., Hoskere, S.N., Ewing, R.D., Mayes, R.L., Button, M.R. and Van Volkinburg, D.R. (1997), "Performance of seismically isolated structures in the 1994 Northridge and 1995 Kobe earthquakes", Building to Last, Leon Kempner, Jr. and Colin B. Brown, Editors, *Proc. of Structures Congress XV,* Published by ASCE, 1128-1132.

Chang, K.C., Shen, J., Tsai, M.H. and Lee, G.C. (2000), "Performance of a seismic isolated bridge under near fault earthquake ground motions", *Proc. of the Taiwan-US-Japan Workshop on Seismic Mitigation of Highway Bridges*, Taipei, Taiwan, September 16-18, 2000.

Chen, Q., Douglas, B.M., Maragakis and Buckle, I.G. (1998), "Extraction of nonlinear hysteresis properties of seismically isolated bridges from quick-release field tests", *Technical Report MCEER-98-0001*, Multidisciplinary Center for Earthquake Engineering Research, State University of New York at Buffalo, Buffalo, New York, May 1998.

Chopra, A.K. (1995), *Dynamics of Structures: Theory and Applications to Earthquake Engineering*. Prentice-Hall, Inc., Englewood Cliffs, N.J.

Clough, R.W. and Penzien, J. (1993), *Dynamics of Structures*. McGraw-Hill, Inc., New York, N.Y.

Gilani, A.S., Mahin, S.A., Fenves, G.L., Aiken, I.D. and Chavez, J.W. (1995), "Field testing of bridge design and retrofit concept, Part 1 of 2: Field testing and computer analysis of a four-span seismically isolated viaduct in walnut creek, California", *Report No. EERC-95/14*, Earthquake Engineering Research Center, University of California at Berkeley, Berkeley, California, December 1995.

Hwang, J.S. Chiou, J.M., Sheng, L.H. and Gates, J.H. (1995), "A refined model for base-isolated bridges with bi-linear hysteresis bearings", *Earthquake Spectra*, **12**(2), 245-274.

Hwang, J.S., Chang, K.C. and Tsai, M.H. (2000), "Design, field testing and seismic performance of a seismically isolated concrete bridge", *Proc. of Canada-Taiwan Workshop on Highway Bridge*, Banf, Canada, 2000.

Ronson, B.N. and Hark, I.E. (1998), "Pullback testing of seismically isolated P/C I-girder bridge", *J. Struct. Eng.*, ASCE, **124**(8), 930-937.

SAP2000, *Integrated Finite Element Analysis and Design of Structures*, Computers and Structures, Inc., 1995 University Avenue, Berkeley, California 94704, USA.

Wendichansky, D.A. (1996), "Experimental investigation of the dynamic response of two bridges before and after retrofitting with elastometric bearings", Ph.D. Dissertation, Civil Engineering Department, State University of New York at Buffalo.